Ultra-high-energy cosmic rays: Anisotropies and potential origins

Alena Bakalová
FZU – Institute of Physics of the Czech Academy of Sciences

21.3.2024

Cosmic rays

- Charged particles coming from outer space
- Steep energy spectrum $\propto E^{-\gamma}, \gamma \sim 3$
- Changes in the spectral index might point to a physics behind their origin
  - Knee (2nd knee)
  - Ankle
  - Suppression
- Ultra-high-energy cosmic rays (UHECRs) $E > 10^{18}$ eV
- Interactions in the atmosphere lead to the creation of extensive air showers of secondary particles
  - Ultra-high energies - showers at ground many km^2

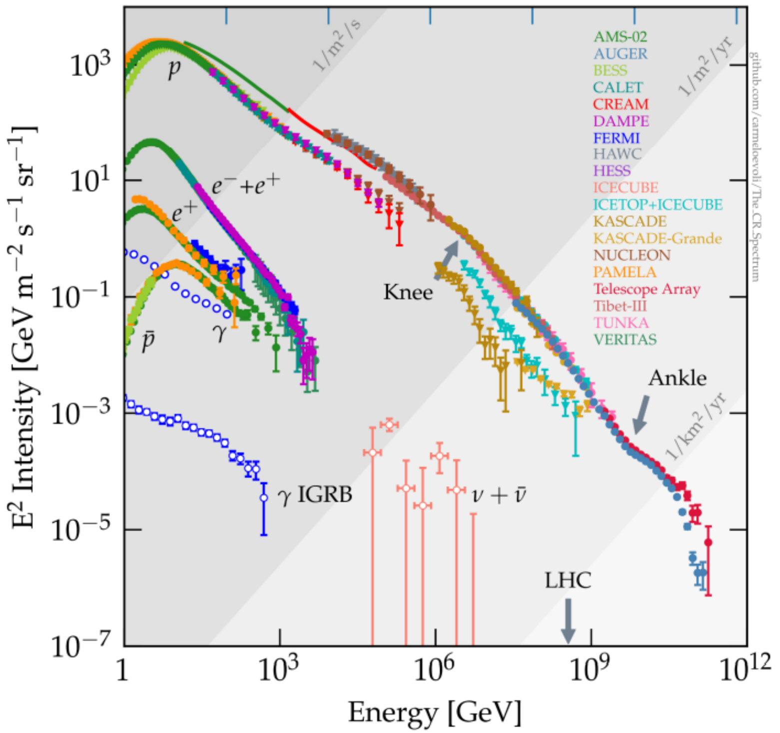

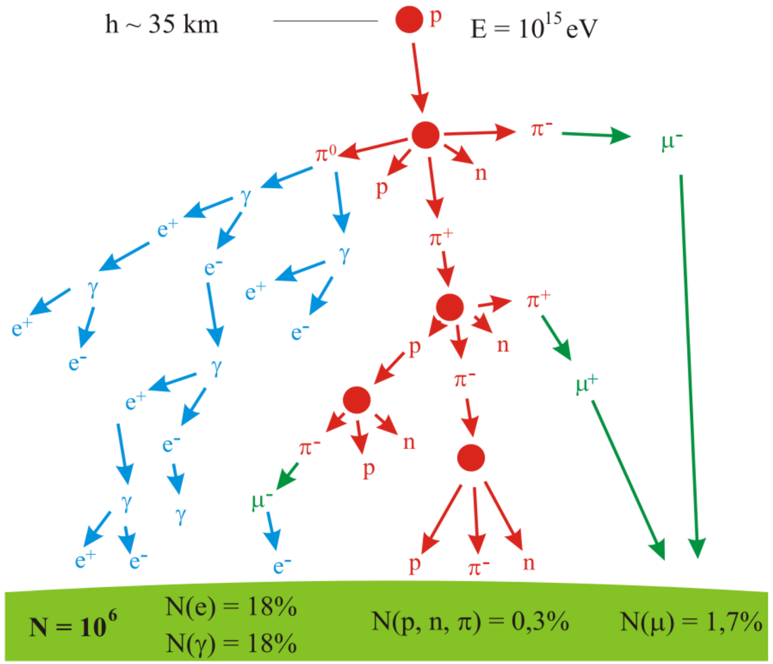

Detecting UHECRs

Pierre Auger Observatory

- Argentina, 3000 km^2
- Operating since 2004
- Recently finished an upgrade of the observatory – phase II

Telescope Array

- Utah, USA
- 700 km^2
- Upgrade to TAx4

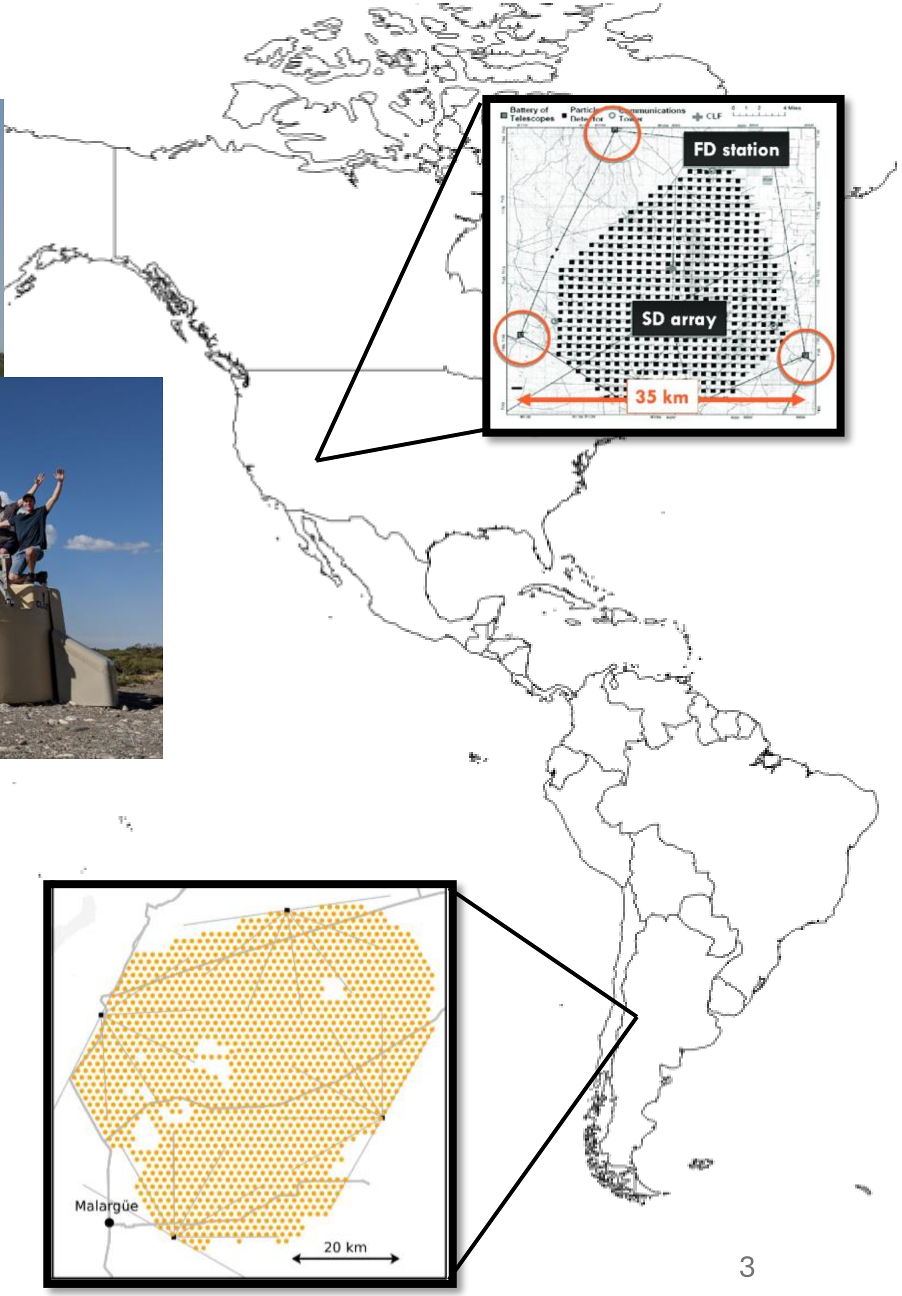

Energy spectrum

- Precise measurements of the energy spectrum at the highest energies
- Pierre Auger Obsrvatory and Telescoep Array energy spectra show differences above few 10^{19} eV
  - Instrument effects? Different models for fluorescence yield? Different sources visible in the Southern and Northern hemisphere? ...

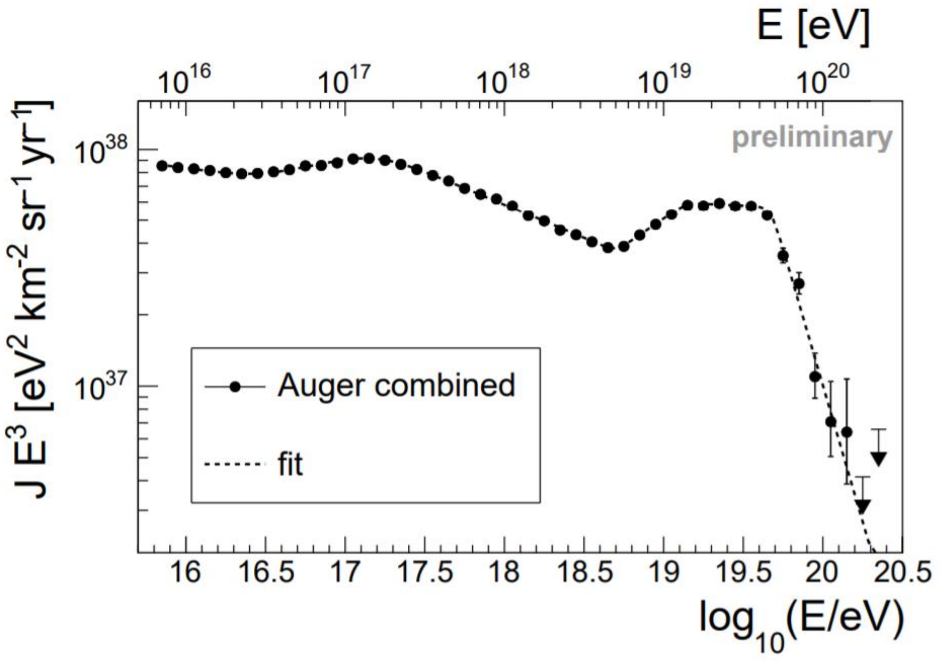

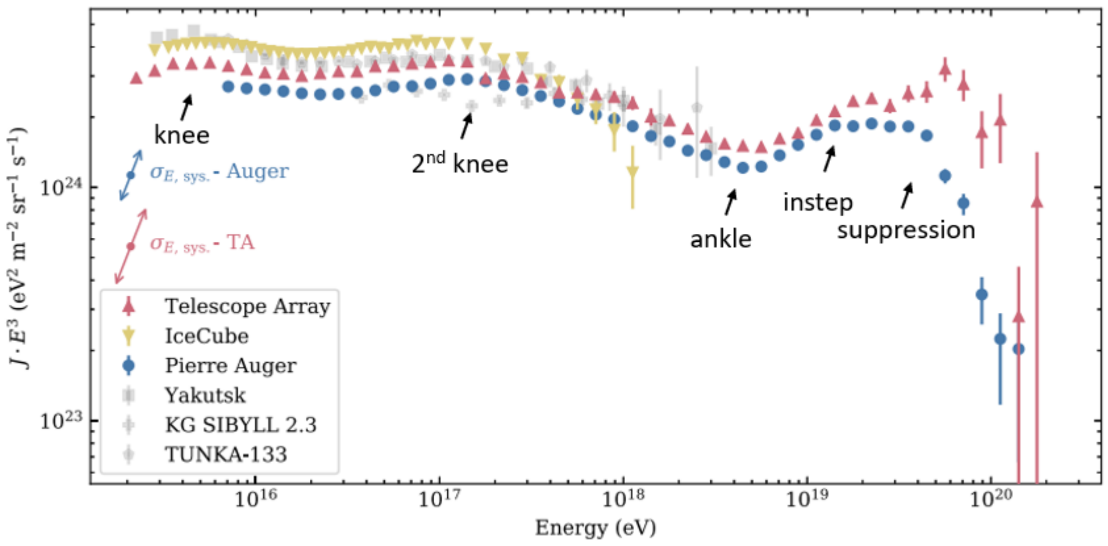

Energy spectrum

→ differences between Auger and TA energy spectra can be reduced by applying energy dependent shift and rescaling of the energy by $\pm 4.5\%$

$\pm 10\% \times \log_{10}(E/10^{19}\mathrm{eV})$

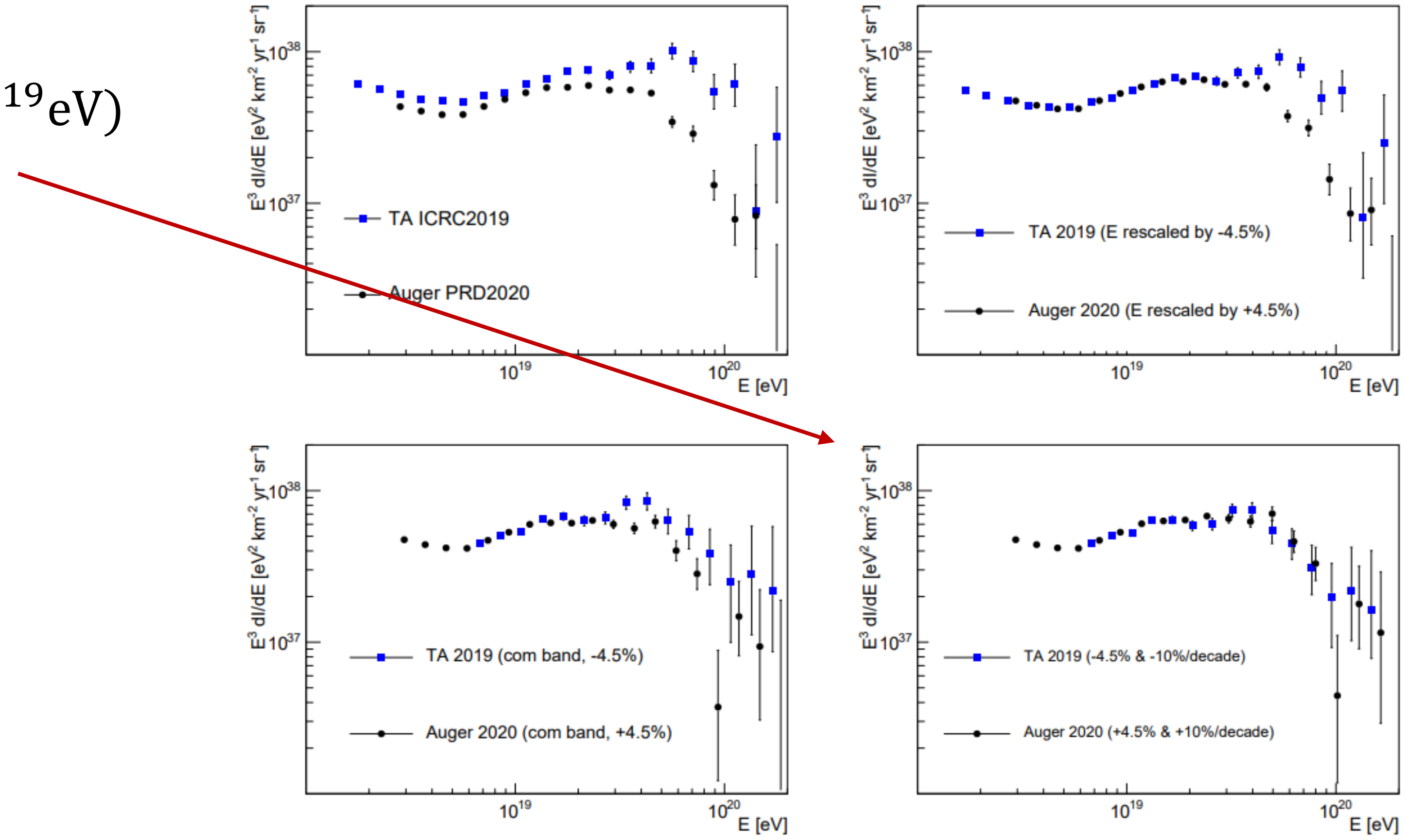

Mass composition

- Indirect measurement from shower parameters
- Most commonly used mass sensitive parameter is shower maximum
- Can not distinguish mass composition on event-by-event basis – statistical distribution
- Large dependence on the models of hadronic interactions

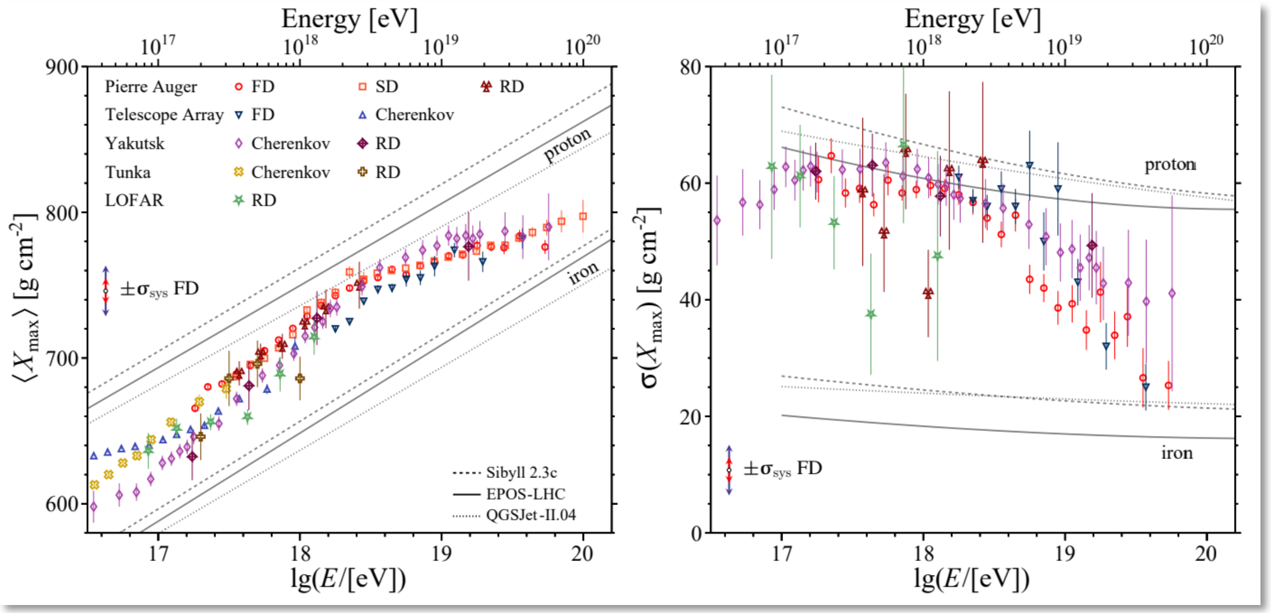

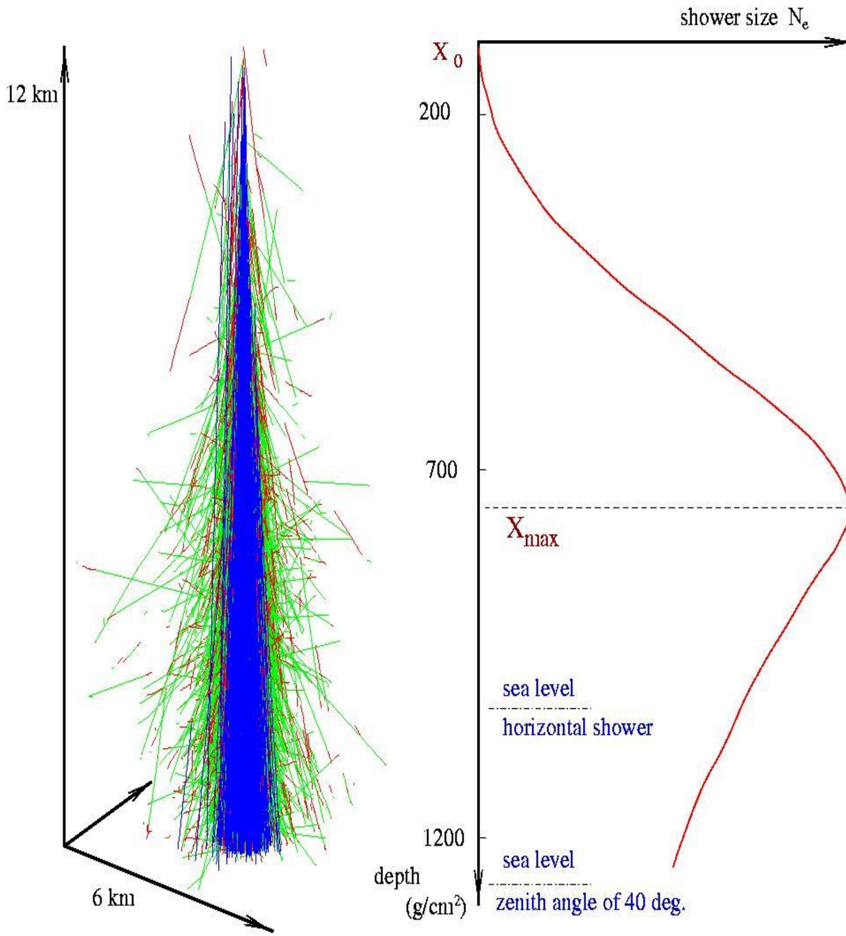

Propagation in the Universe: Particle interactions

- Cosmic rays can interact with ambient photon fields and matter particles in the universe
- Mostly interactions on CMB
  - ***Photo-pion production***

$$p + \gamma \rightarrow \Delta^+ \rightarrow \begin{matrix} p + \pi^0 \\ n + \pi^+ \end{matrix} \quad , \quad E_{th} \cong 6.8 \cdot 10^{19} \left(\frac{\epsilon}{10^{-3}\ \text{eV}} \right)^{-1} \text{eV}$$

  - ***Electron pair production***

$$E_{th} \cong 4.8 \cdot 10^{17} A \left(\frac{\epsilon}{10^{-3}\ \text{eV}} \right)^{-1} \text{eV}$$

  - ***Photodisintegration*** – changes both energy and mass composition of cosmic rays, main energy loss process for heavier nuclei
- Nuclear decay, cosmological redshift, interactions with matter ...

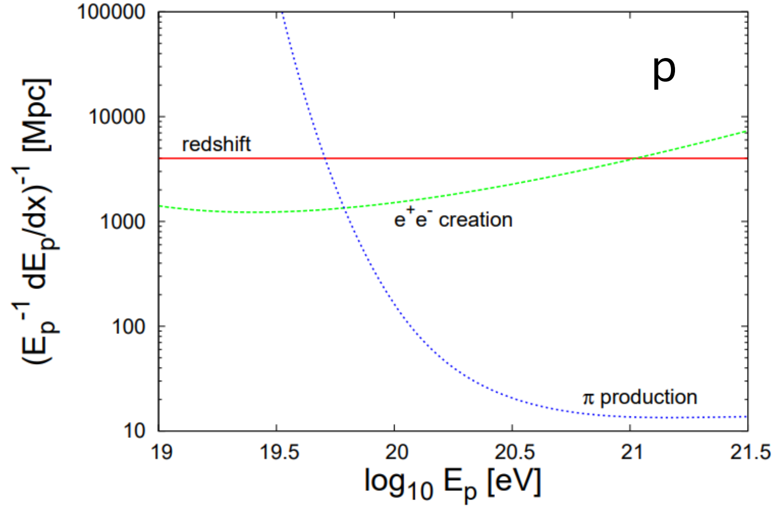

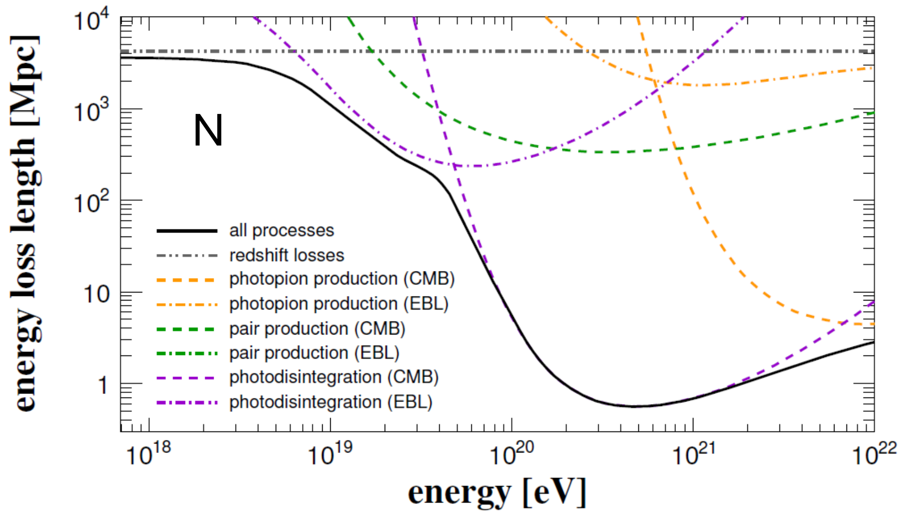

Propagation in the Universe: Deflections in magnetic fields

- Cosmic rays are charged – trajectories influenced by magnetic fields in the universe -
  - **Extragalactic magnetic fields** are not known in large detail – weak but long trajectories
  - **Galactic magnetic field** – better mapped, strength few tens of μG

To track cosmci rays back to their sources we need high energy light particles!

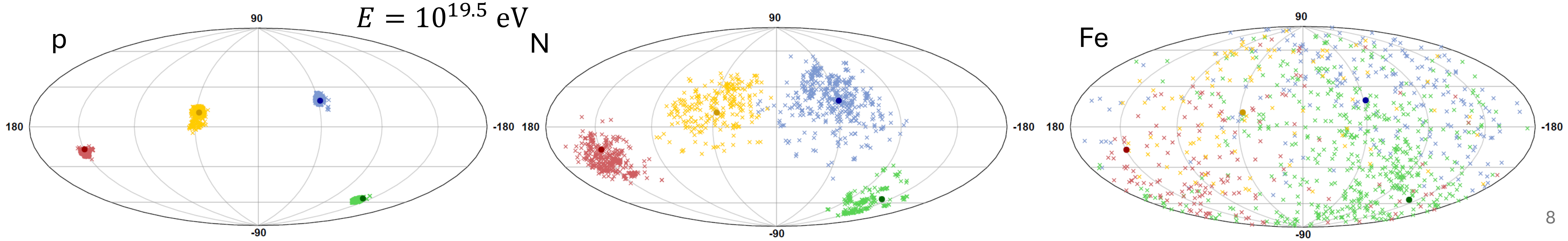

Propagation in the Universe: Deflections in magnetic fields

- Cosmic rays are cha… c fields in the universe
  - **Extragalactic magn…** …out long trajectories
  - **Galactic magnetic f…**

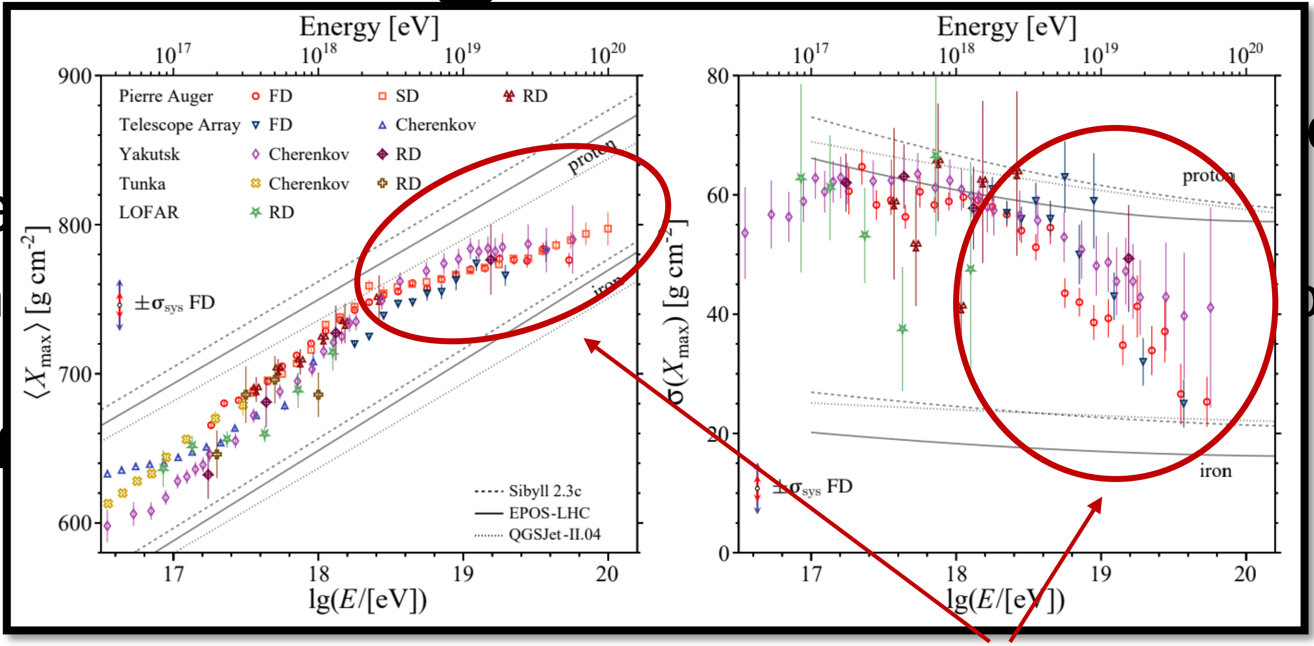

To track cosmic rays back to their sources we need high energy light particles!

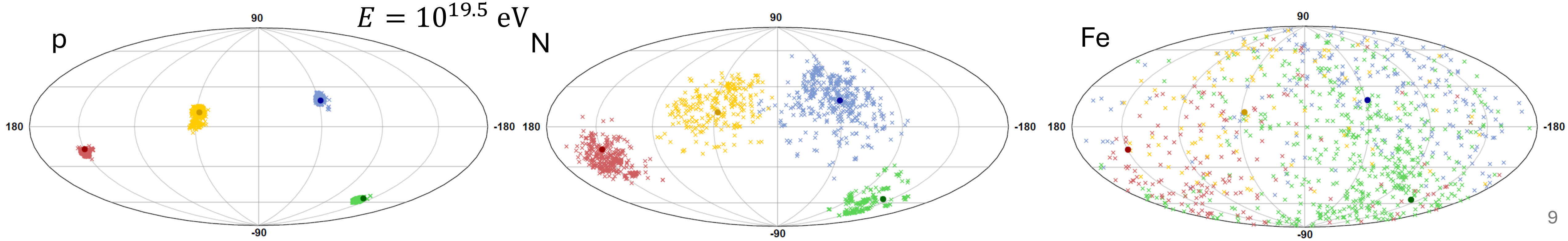

Anisotropies in arrival directions

Blind searches for excesses at the Pierre Auger Observatory

- Largest signal found for $E > 41$ EeV with top-hat smoothing 24° in coordinates $(l, b) = (305.4°,\ 16.2°)$
- 153 observed events 97.7 expected from isotropy
- Hotspot located 2.9° from NGC 4945 and 5.1° from Centaurus A

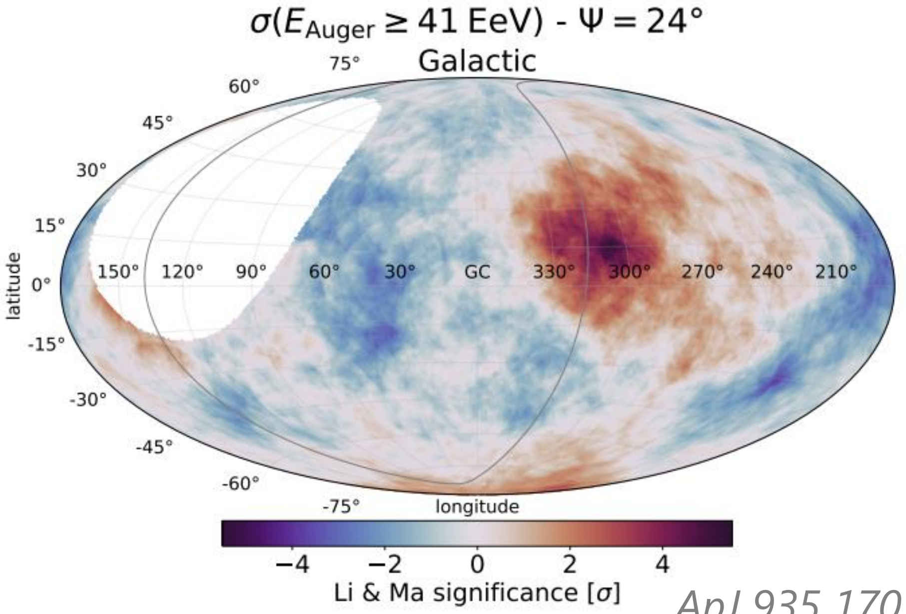

ApJ 935 170 (2022)

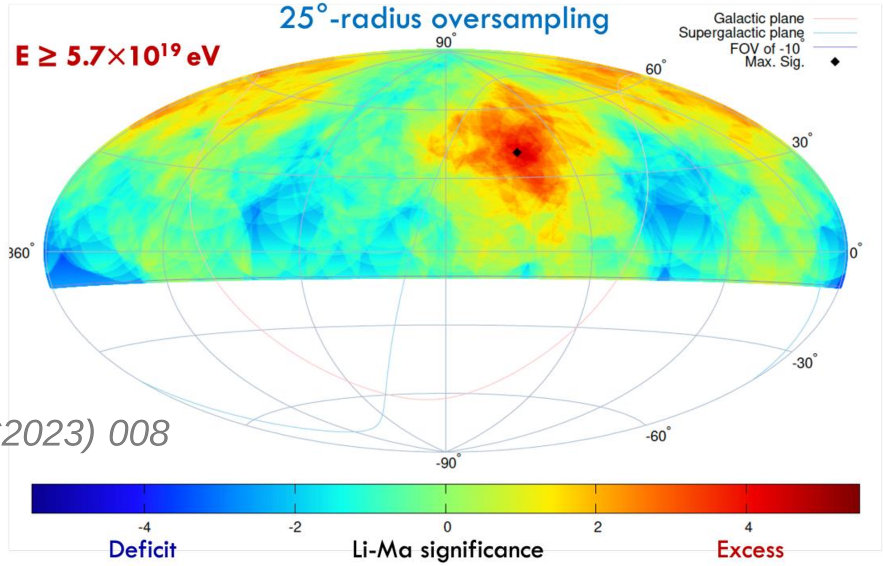

PoS(ICRC2023) 008

Blind searches for excesses at Telescope Array

- Hotspot
  - For $E > 57$ EeV at $(\alpha, \delta) = (144°, 40.5°)$
  - 44 observed events vs. 18 expected from isotropy
- Perseus-Pisces supercluster excess
  - For $E > 25$ EeV at $(\alpha, \delta) = (17.9°, 35.2°)$

Anisotropies in arrival directions

Correlation with catalogues with the Pierre Auger Observatory data

- 2MASS Redshift Survey of near infrared galaxies
- Starburst galaxies
- X-ray AGNs from Swift-BAT catalogue
- γ-ray AGNs from Fermi-LAT catalogue

$\rightarrow$ 2 peak structure ~ 40 EeV and ~ 60 EeV

Catalog	E_{th} [EeV]	Fisher search radius, Θ [deg]	Signal fraction, α [%]	TS_{max}	Post-trial p-value
All galaxies (IR)	40	16^{+11}_{-6}	16^{+10}_{-7}	18.0	7.9×10^{-4}
Starbursts (radio)	38	15^{+8}_{-4}	9^{+6}_{-4}	25.0	3.2×10^{-5}
All AGNs (X-rays)	39	16^{+8}_{-5}	7^{+5}_{-3}	19.4	4.2×10^{-4}
Jetted AGNs (γ-rays)	39	14^{+6}_{-4}	6^{+4}_{-3}	17.9	8.3×10^{-4}
All galaxies (IR)	58	14^{+9}_{-5}	18^{+13}_{-10}	9.8	2.9×10^{-2}
Starbursts (radio)	58	18^{+11}_{-6}	19^{+20}_{-9}	17.7	9.0×10^{-4}
All AGNs (X-rays)	58	16^{+8}_{-6}	11^{+7}_{-6}	14.9	3.2×10^{-3}
Jetted AGNs (γ-rays)	58	17^{+8}_{-5}	12^{+8}_{-6}	17.4	1.0×10^{-3}

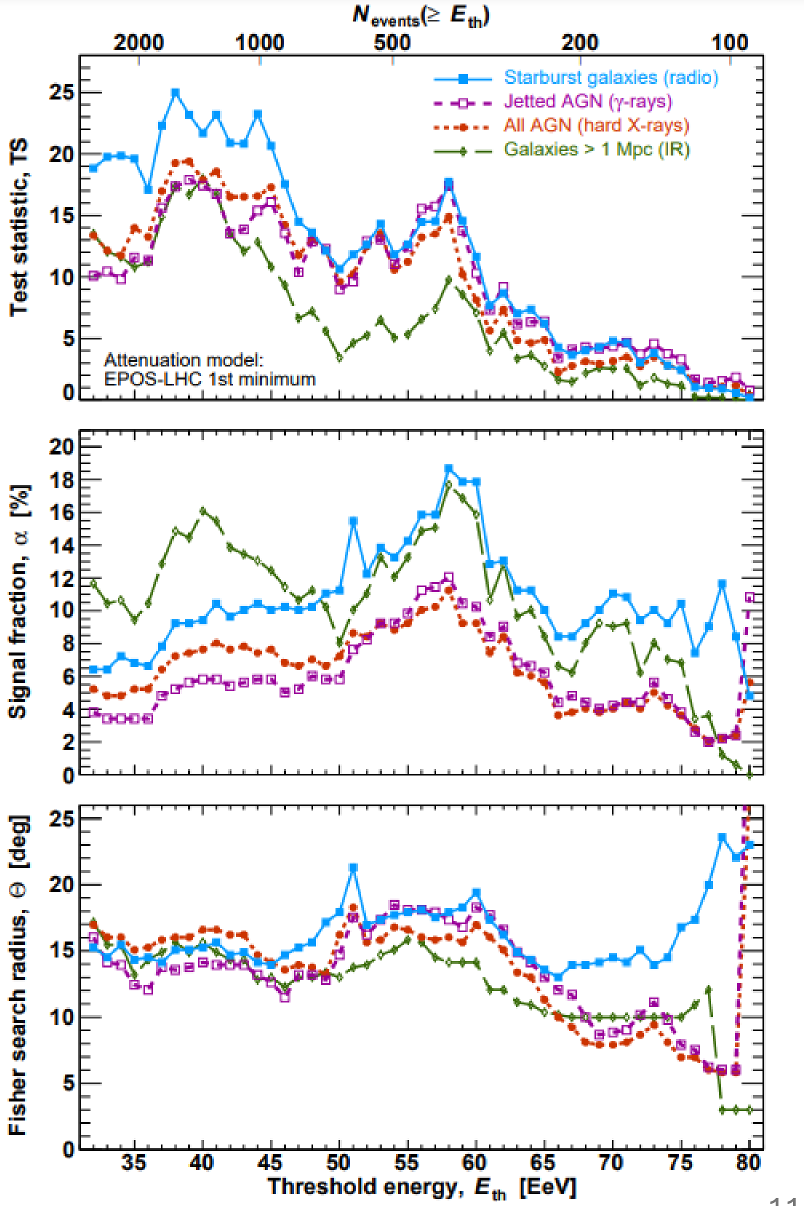

ApJ 935 170 (2022)

Anisotropies in arrival directions

Targeted search – ***Centaurus A*** region

- Closest radio galaxy to Earth ~3.7 Mpc, NGC 4945, M83
- Enhanced flux in all four studied catalogues
- Energy above 38 EeV and window of 27°
- 215 events observed vs 152 expected from isotropy → 3.9σ

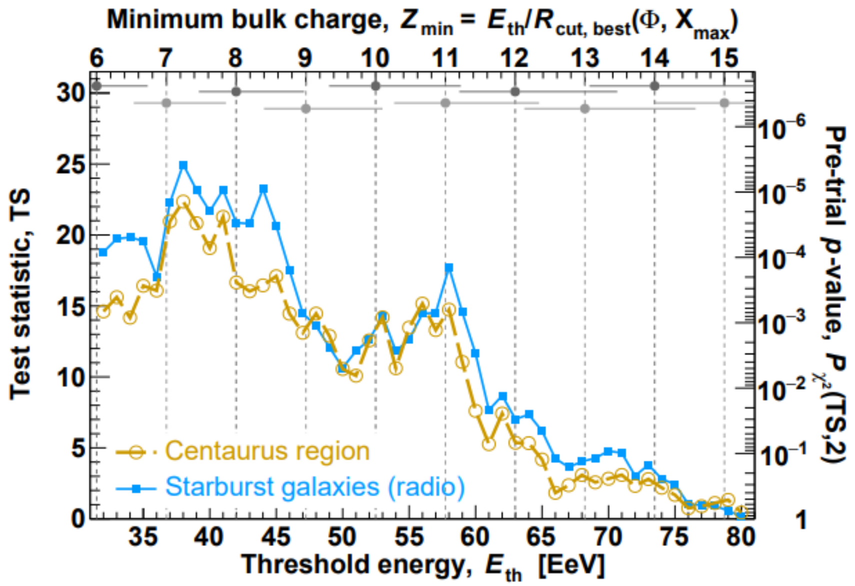

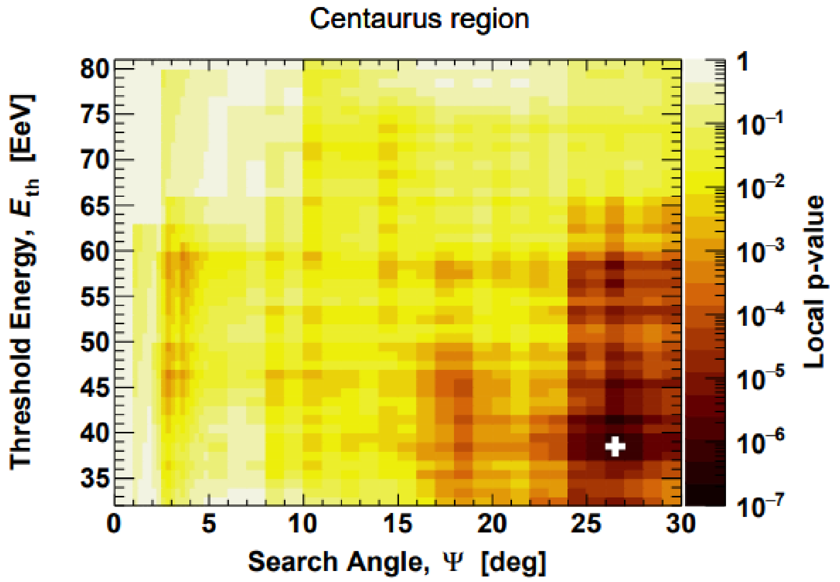

ApJ 935 170 (2022)

Large scale anisotorpies - dipole

- Dipole in the arrival directions of cosmic rays above 8 EeV
- Points ~125° from the Galactic center - suggests an **extragalactic origin**
- Amplitude $6.5^{+1.3}_{-0.9}$ %, direction $(l, b) = (233°, -13°)$ and significance over 6σ
- Amplitude evolves with energy

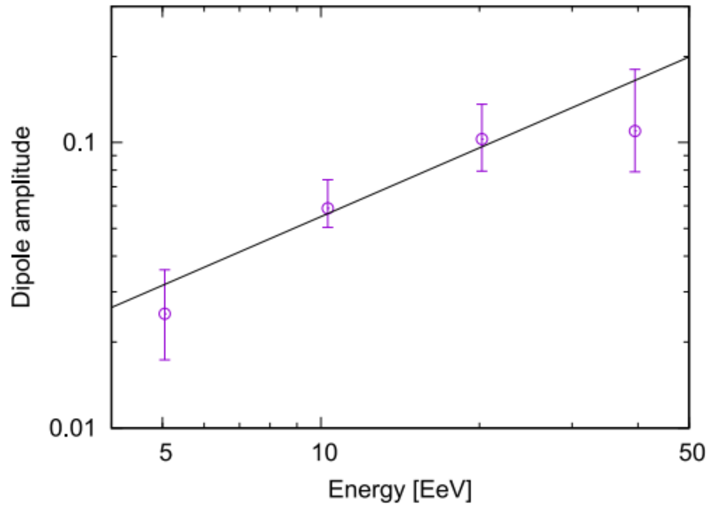

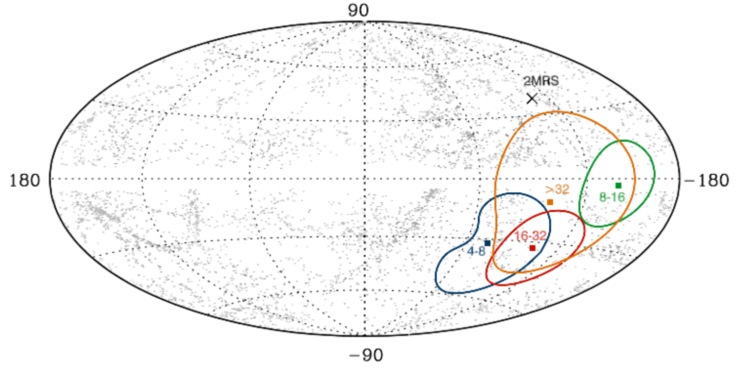

ApJ 868 (2018) 4

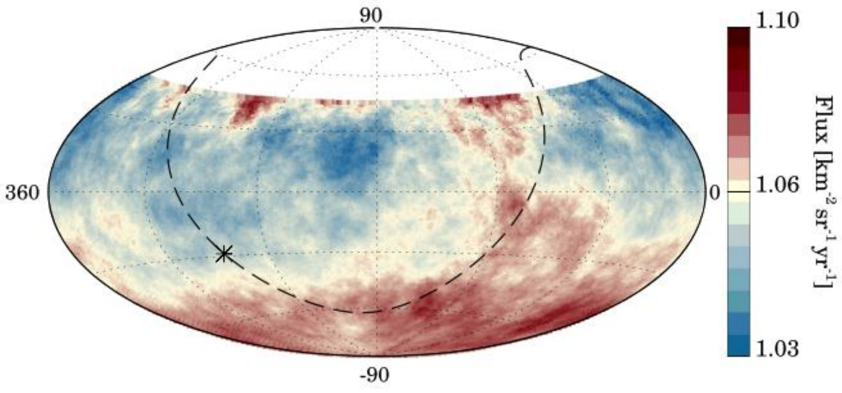

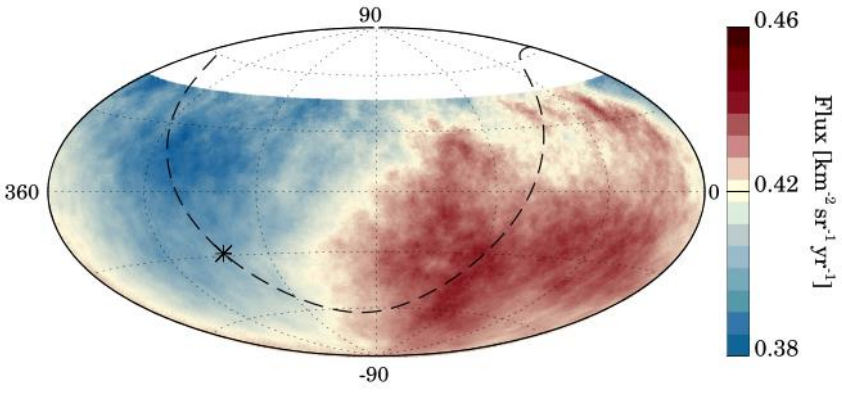

ApJ 868 (2018) 4

Large scale anisotorpies - dipole

- Arrival directions analyzed for dipole and quadrupole anisotropies – most significant dipole above 8 EeV

$$\phi(\hat{u}) = \frac{\phi_0}{4\pi}\left(1 + d \cdot \hat{u} + \frac{1}{2}\sum_{i,j} Q_{i,j}\, u_i u_j\right)$$

- Joint analysis - **Auger and TA**

energies (Auger)	[8.57 EeV, 16 EeV)	[16 EeV, 32 EeV)	[32 EeV, +∞)
energies (TA)	[10 EeV, 19.47 EeV)	[19.47 EeV, 40.8 EeV)	[40.8 EeV, +∞)
d_x [%]	−0.7 ± 1.1 ± 0.0	+1.6 ± 2.0 ± 0.0	−5.3 ± 3.9 ± 0.1
d_y [%]	+4.8 ± 1.1 ± 0.0	+3.9 ± 1.9 ± 0.1	+9.7 ± 3.7 ± 0.0
d_z [%]	−3.3 ± 1.4 ± 1.3	−6.0 ± 2.4 ± 1.3	+3.4 ± 4.7 ± 3.6
$Q_{xx} - Q_{yy}$ [%]	−5.1 ± 4.8 ± 0.0	+13.6 ± 8.3 ± 0.0	+43 ± 16 ± 0
Q_{xz} [%]	−3.9 ± 2.9 ± 0.1	+5.4 ± 5.1 ± 0.0	+5 ± 11 ± 0
Q_{yz} [%]	−4.9 ± 2.9 ± 0.0	−9.6 ± 5.0 ± 0.1	+11.9 ± 9.8 ± 0.2
Q_{zz} [%]	+0.5 ± 3.3 ± 1.7	+5.2 ± 5.8 ± 1.7	+20 ± 11 ± 5
Q_{xy} [%]	+2.2 ± 2.4 ± 0.0	+0.2 ± 4.2 ± 0.1	+4.5 ± 8.1 ± 0.1
C_1 [10^{-3}]	4.8 ± 2.0 ± 1.2	7.6 ± 4.6 ± 2.2	19 ± 12 ± 4
C_2 [10^{-3}]	0.85 ± 0.66 ± 0.02	3.1 ± 2.2 ± 0.2	15.5 ± 8.9 ± 2.4

PoS(ICRC2021) ***395*** *375*

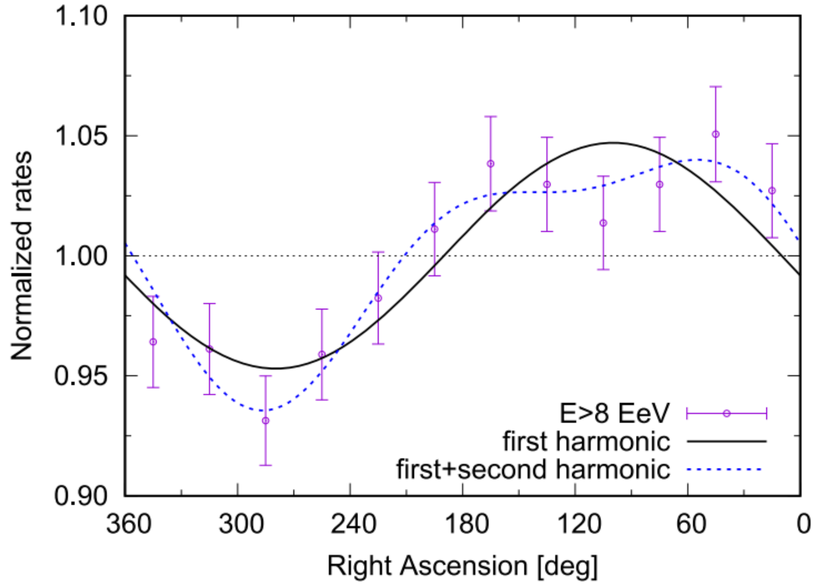

ApJ 868 (2018) 4

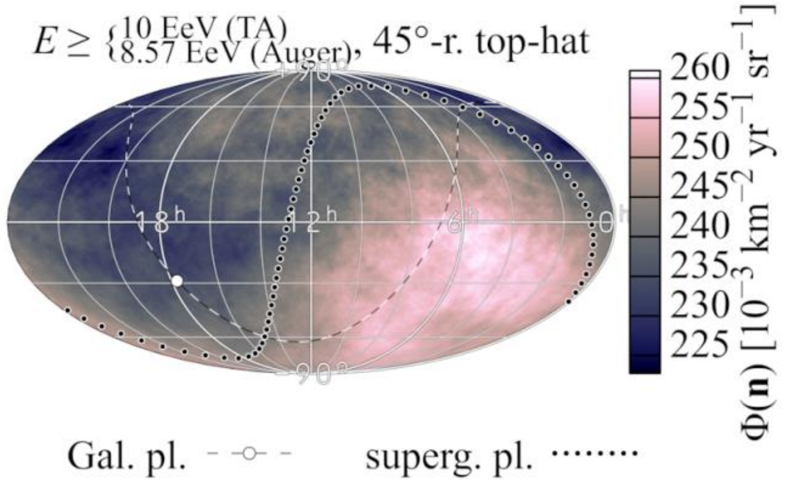

PoS(ICRC2021) 375

Influence of the Galactic magnetic field

- Cosmic rays are charged particles → trajectories are deflected in Galactic magnetic field (GMF) and extragalactic magnetic field (EGMF)
- Deflections depend on particle energy E and charge Z → rigidity $R = E/Z$

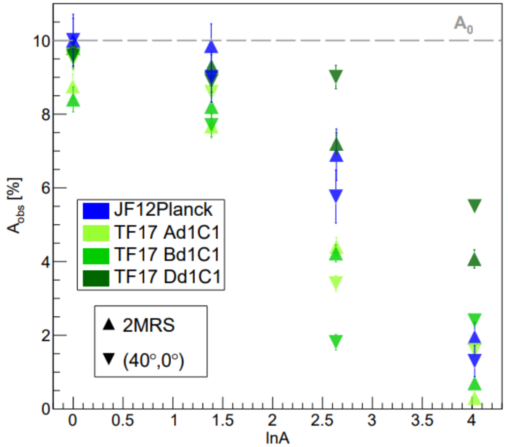

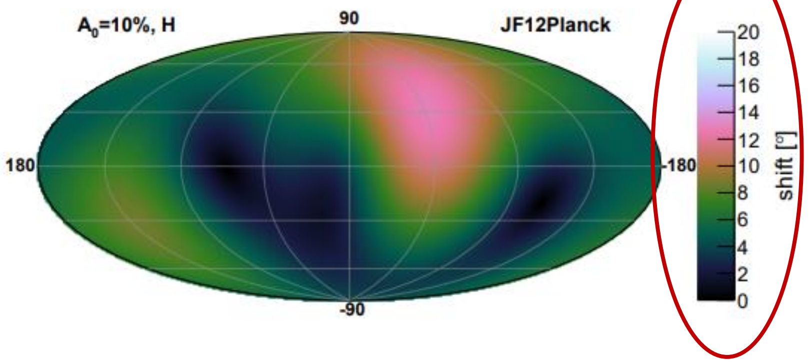

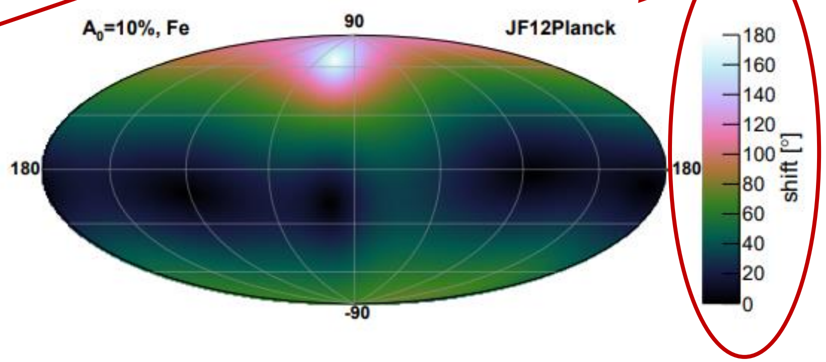

- GMF can change the direction of the dipole and also its amplitude

What can we say about the UHECR dipole before cosmic rays enter the Galactic magnetic field?

A. Bakalová *et al* JCAP12(2023)016

Simulations of cosmic ray propagation

- Isotropic flux of cosmic rays propagated in the GMF using multiple models of GMF used
  - **JF12Planck model of GMF**
    - In order to include uncertainties of the field different coherence lengths of the turbulent component used: 30 pc, 60 pc and 100 pc
  - **TF17 model of GMF**
    - Three options of the field used: Ad1C1, Bd1C1, Dd1C1
    - Results checked with field strength adjusted by $\pm 10\%$

- Four types of primary particles simulated separately: p, He, N, Fe
- Power law energy spectrum with spectral index $\gamma = 3$, energy range $(8 - 100)$ EeV
- EGMF and energy losses neglected

Models of GMF

JF12Planck | **TF17: Ad1C1** | **TF17: Bd1C1** | **TF17: Dd1C1**

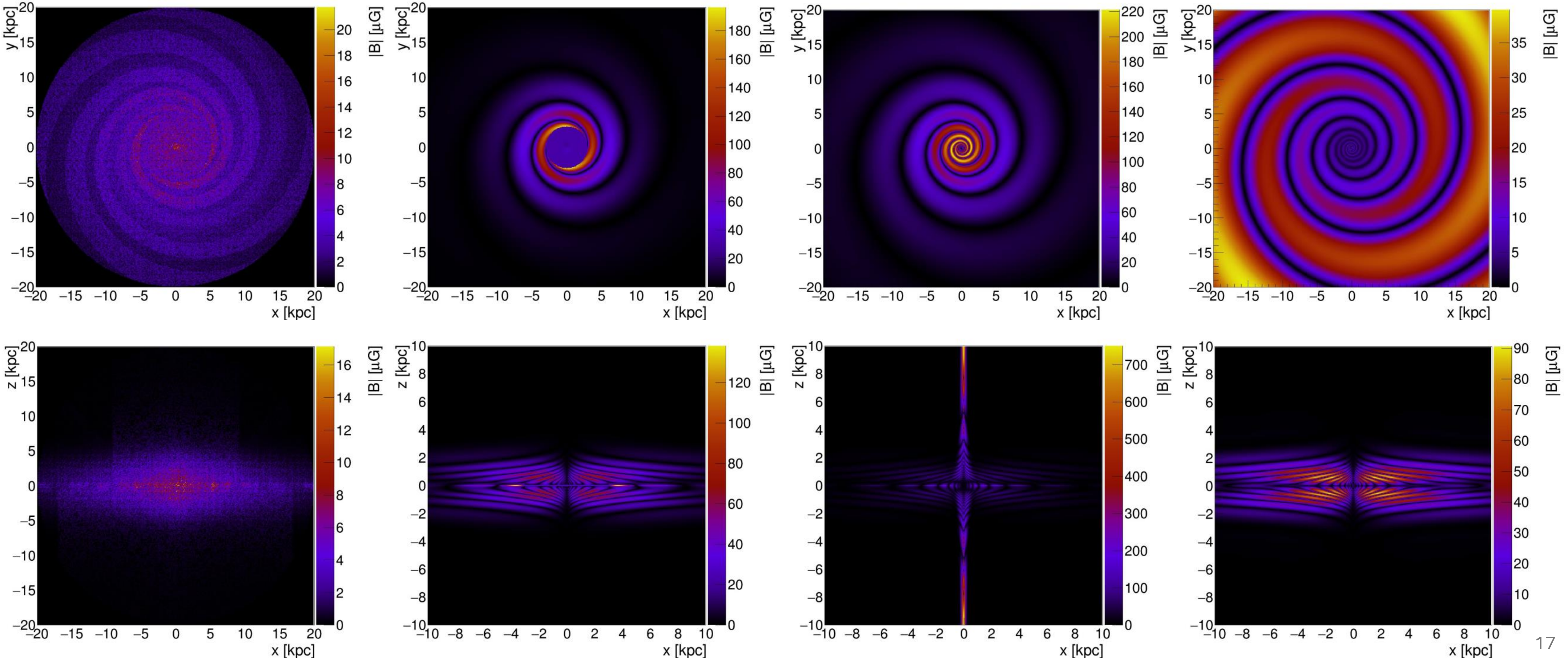

Imposing dipole into the simulated flux

- Simulated particles reweighted according to their original direction on the edge of the Galaxy by

$$w = A_0 \cos \delta + 1$$

δ - angular distance from the direction of the dipole
A_0 - extragalactic amplitude as a percentage of the relative excess with respect to the mean flux

- Dipole injected to all different combinations of galactic longitude and latitude with step of 1° using various amplitudes A_0 in discrete steps from 6.5 % up to 20 %

  → total of 518,400 combinations for each element

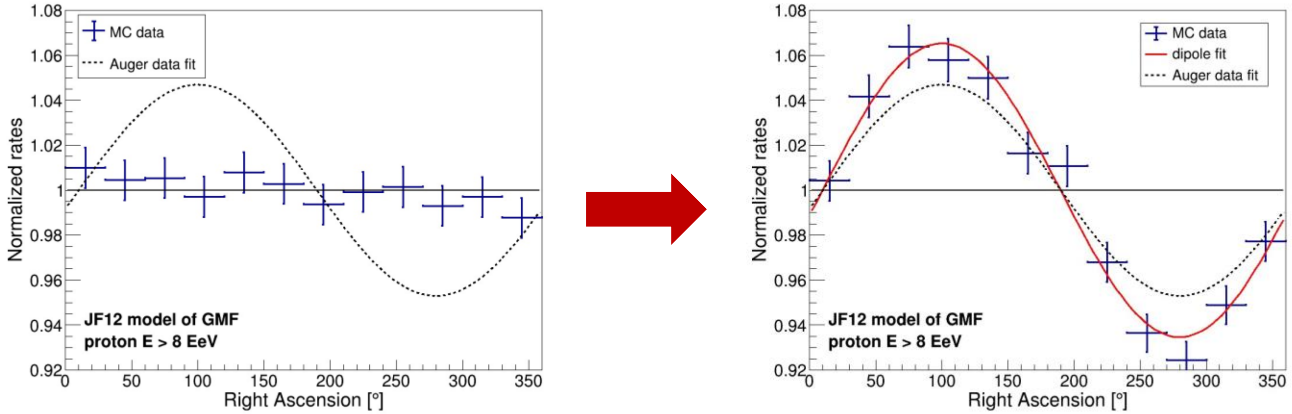

- Mass compositions explored by combining the four elements with a step of 5%

  → 1,771 combinations for the mass composition mixes

Reconstruction of the dipole

- Dipole with unit vector pointing in the direction of the dipole $\boldsymbol{D}$ and amplitude A

$$\Phi(\boldsymbol{u}) = \frac{\Phi_0}{4\pi}(1 + A\boldsymbol{D} \cdot \boldsymbol{u})$$

- Zeroth and first moments of the flux

$$I_0 = \int \Phi(\boldsymbol{u})\mathrm{d}\Omega \;, \qquad \boldsymbol{I} = \int \boldsymbol{u}\Phi(\boldsymbol{u})\mathrm{d}\Omega$$

- We can obtain **dipole amplitude** and **dipole direction** on the observer using discrete versions of these integrals

$$S_0 = \sum_k \frac{1}{w_k}, \qquad \boldsymbol{S} = \sum_k \frac{\boldsymbol{u}_k}{w_k} \longrightarrow A = \frac{3\|\boldsymbol{S}\|}{S_0}, \qquad \boldsymbol{D} = \frac{\boldsymbol{S}}{\|\boldsymbol{S}\|}$$

Looking for parameters of the extragalactic dipole (A_0, D_0) that are compatible after the propagation with the measurements of the Pierre Auger Observatory at the 1σ and 2σ level.

Results for single element scenario

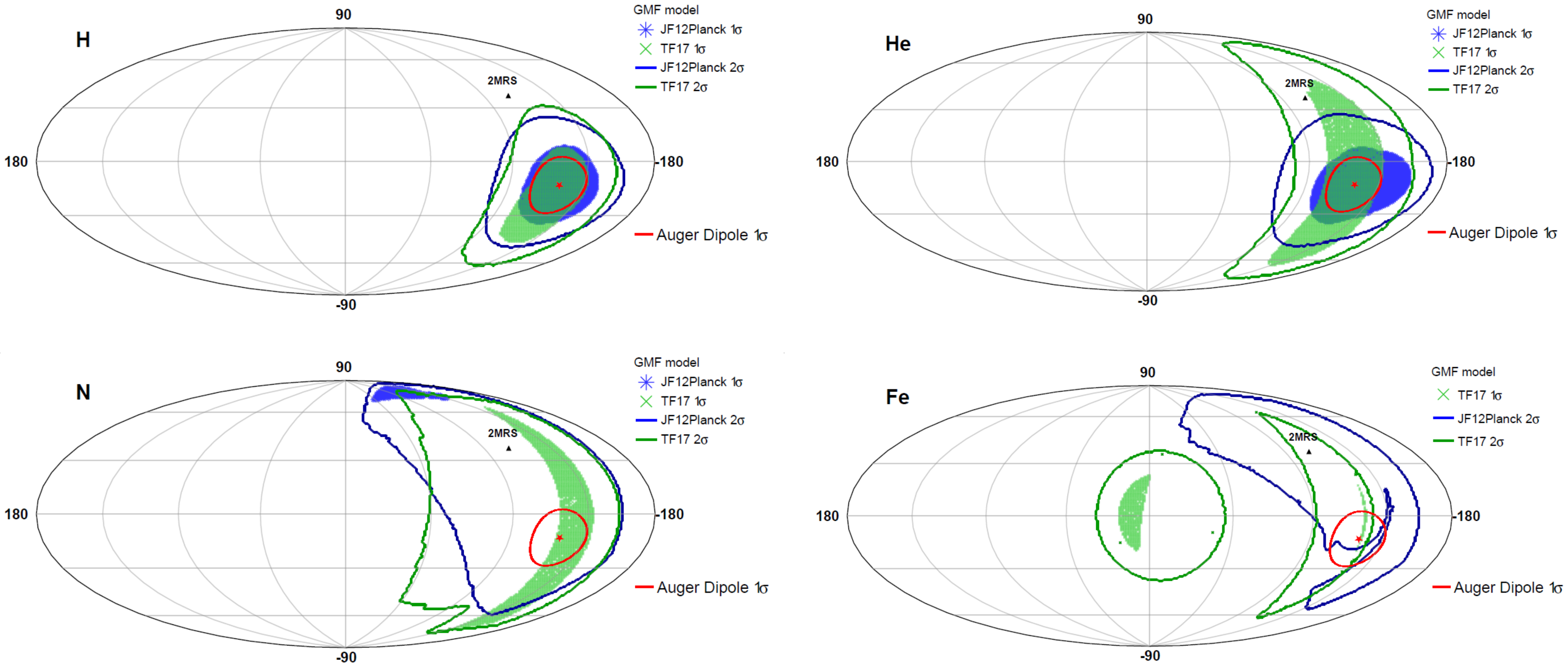

At the 1σ level only TF17 with $A_0 = 20\%$

Results for mixed mass composition

- **JF12Planck** – two groups of solutions at the 1σ level
    1. Within $\approx 45^{\circ}$ from the measured dipole
    2. Up to $\approx 105^{\circ}$ from the measured dipole – nitrogen-dominated composition

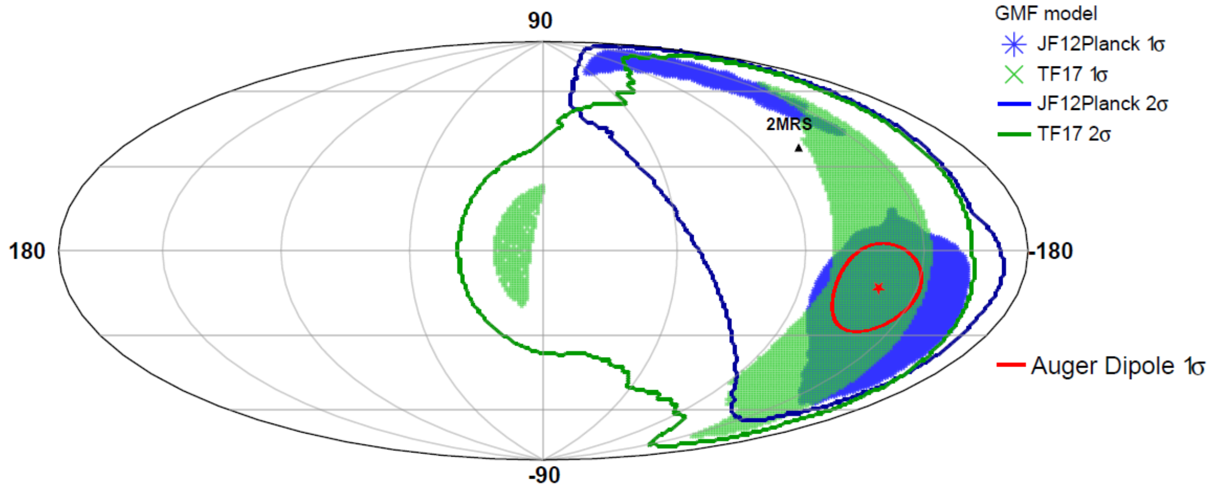

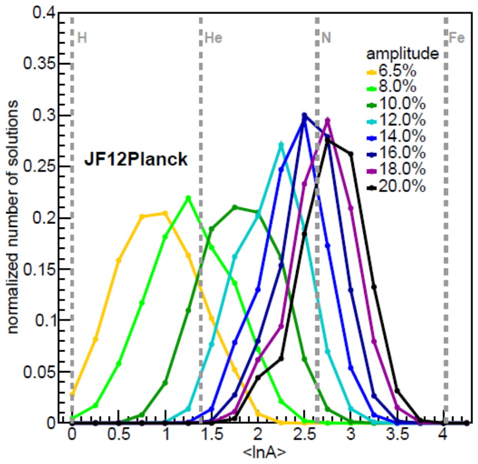

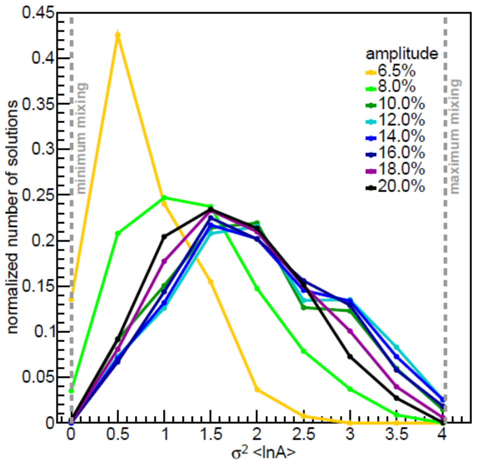

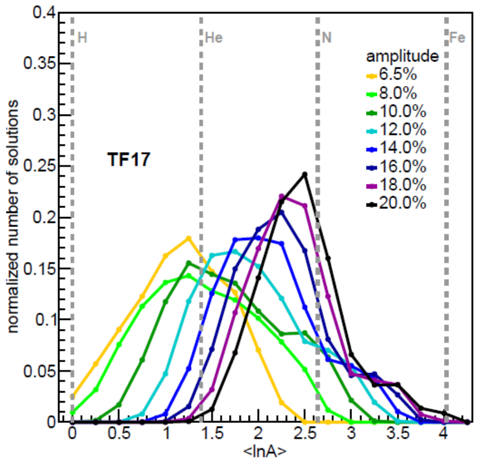

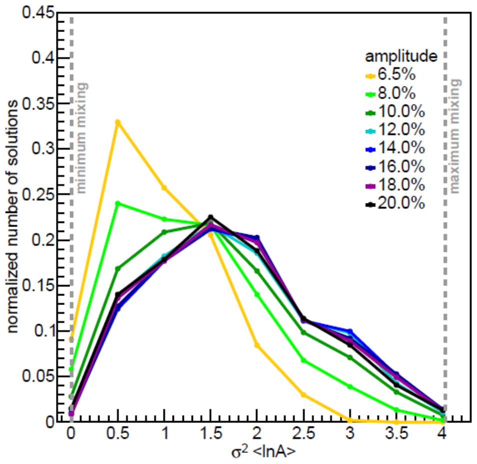

Results for mixed mass composition

- **TF17** – two groups of solutions at the 1σ level
    1. Narrow band of longitudes but a wide range of latitude, within $\approx 80^{\circ}$ from measured dipole
    2. Close to the Galactic center solutions for pure iron nuclei TF17 Bd1C1

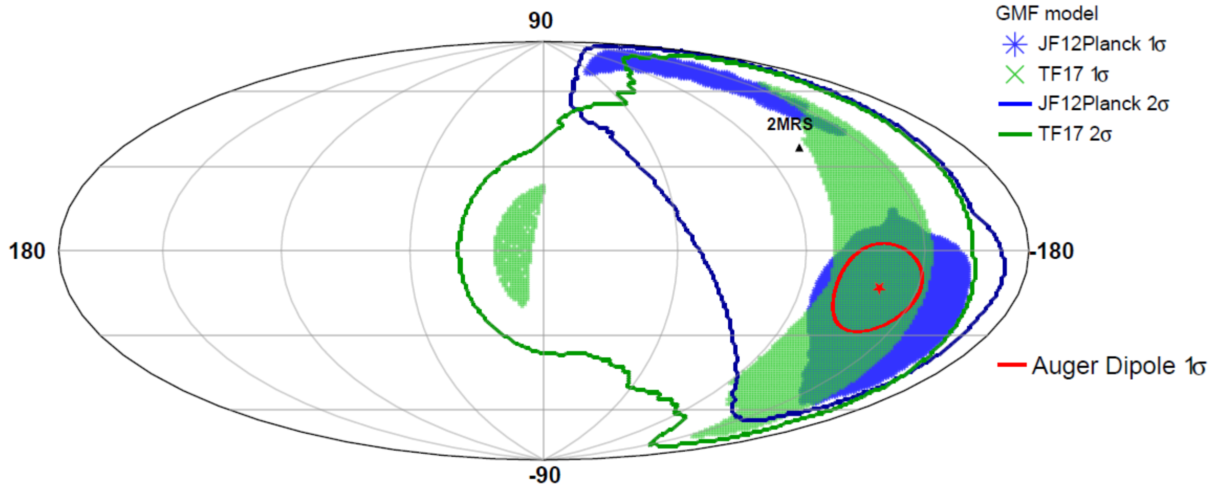

NOT IN CONTRADICTION WITH EXTRAGALCTIC ORIGIN

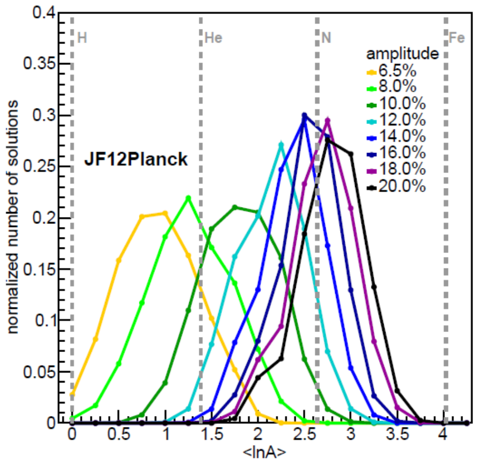

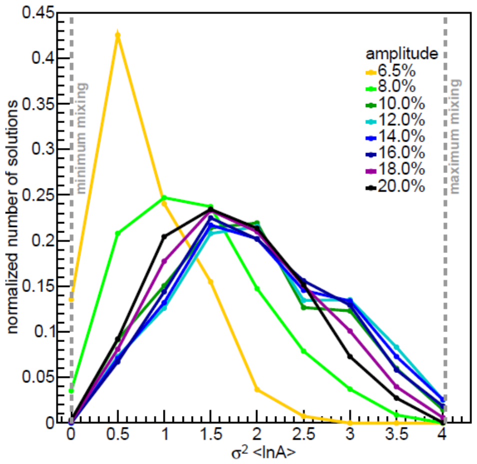

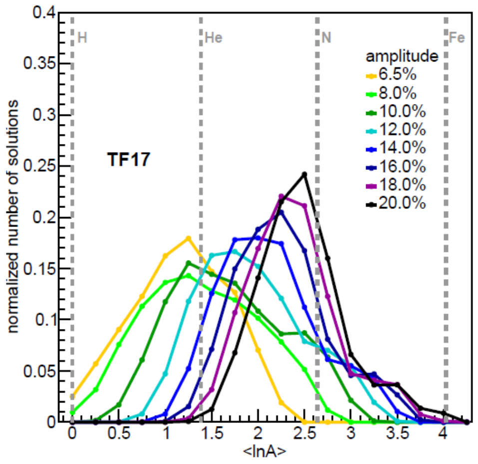

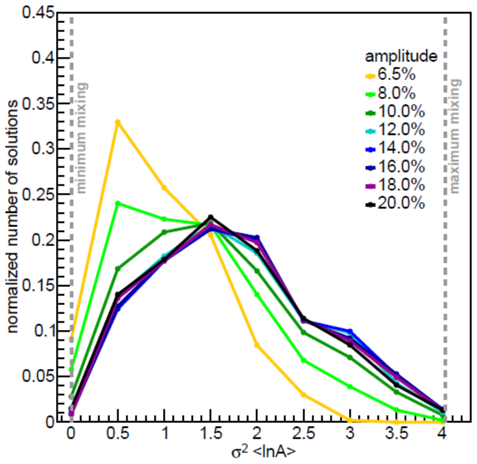

Summary

- Light high energy particles are needed for cosmic ray astronomy
  - Current measurements show cosmic rays are getting heavier at highest energies – new upgraded observatories can help in better identification of the mass of primary particles
- Intermediate scale anisotropies seen in data of the Pierre Auger Obsrvatory and Telescope Array - possible clustering around prominent sources?
- Dipole anisotropy in arrival directions
  - Extragalactic origin
  - Anisotropic distribution of sources
  - Dipole outside the Galaxy can have very different direction and amplitude depending on the mass composition above 8 EeV
  - 2MRS dipole direction compatible with the Auger dipole at the 2σ
- Upgraded observatories will provide new and better data
- New models of magnetic fields can help tracking particles back to their origin

Pierre Auger Observatory

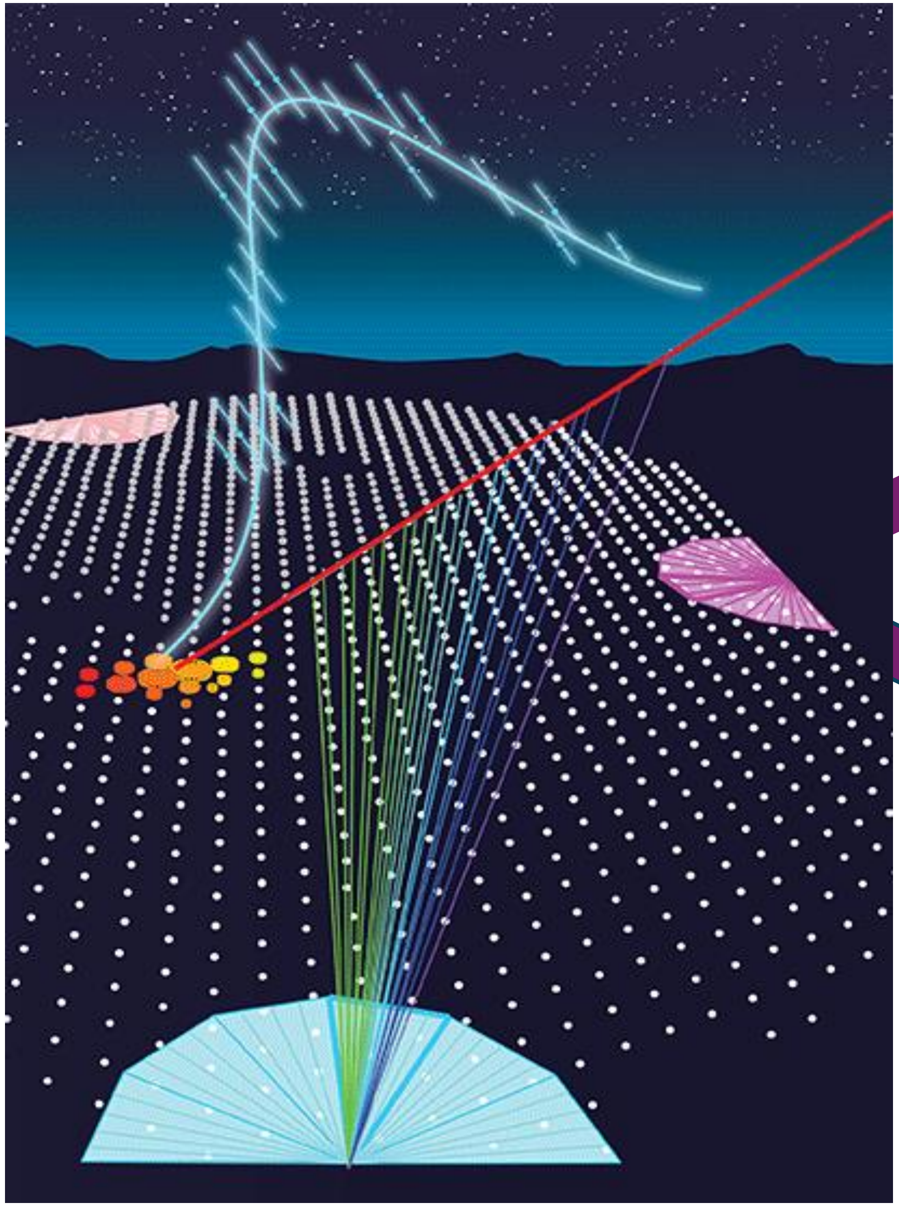

SD

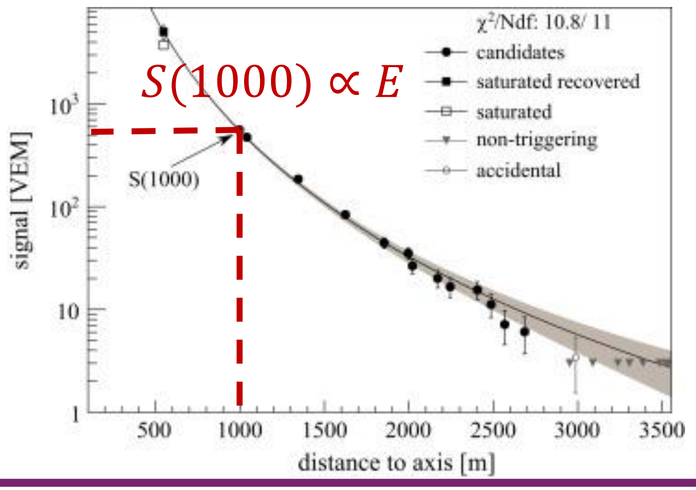

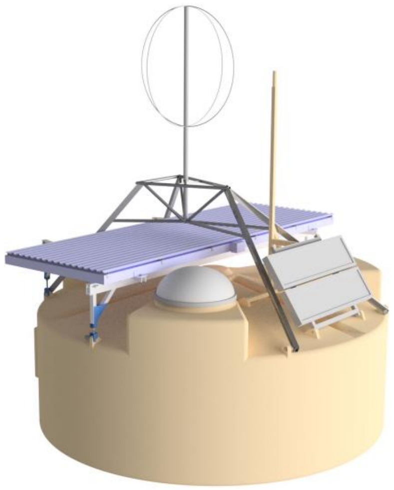

FD

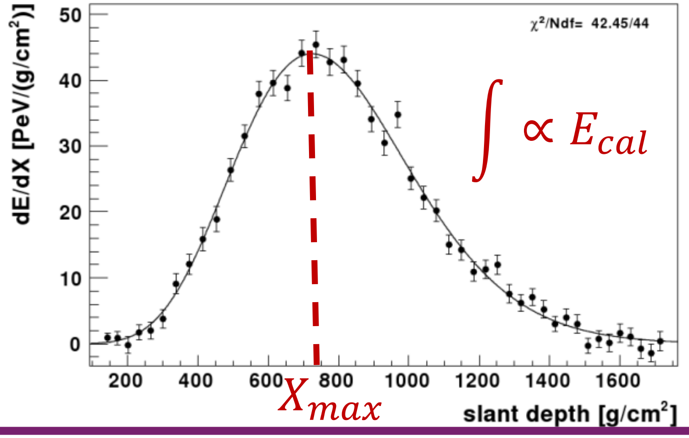

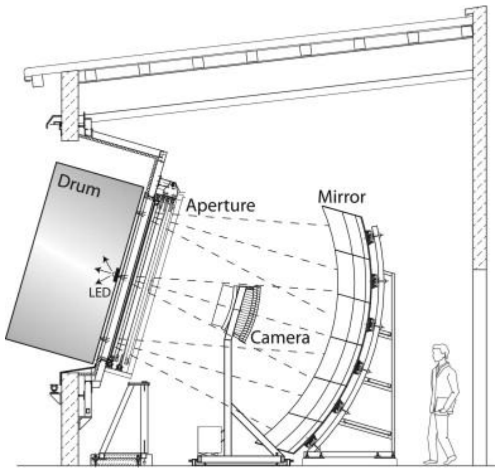

Energy spectrum

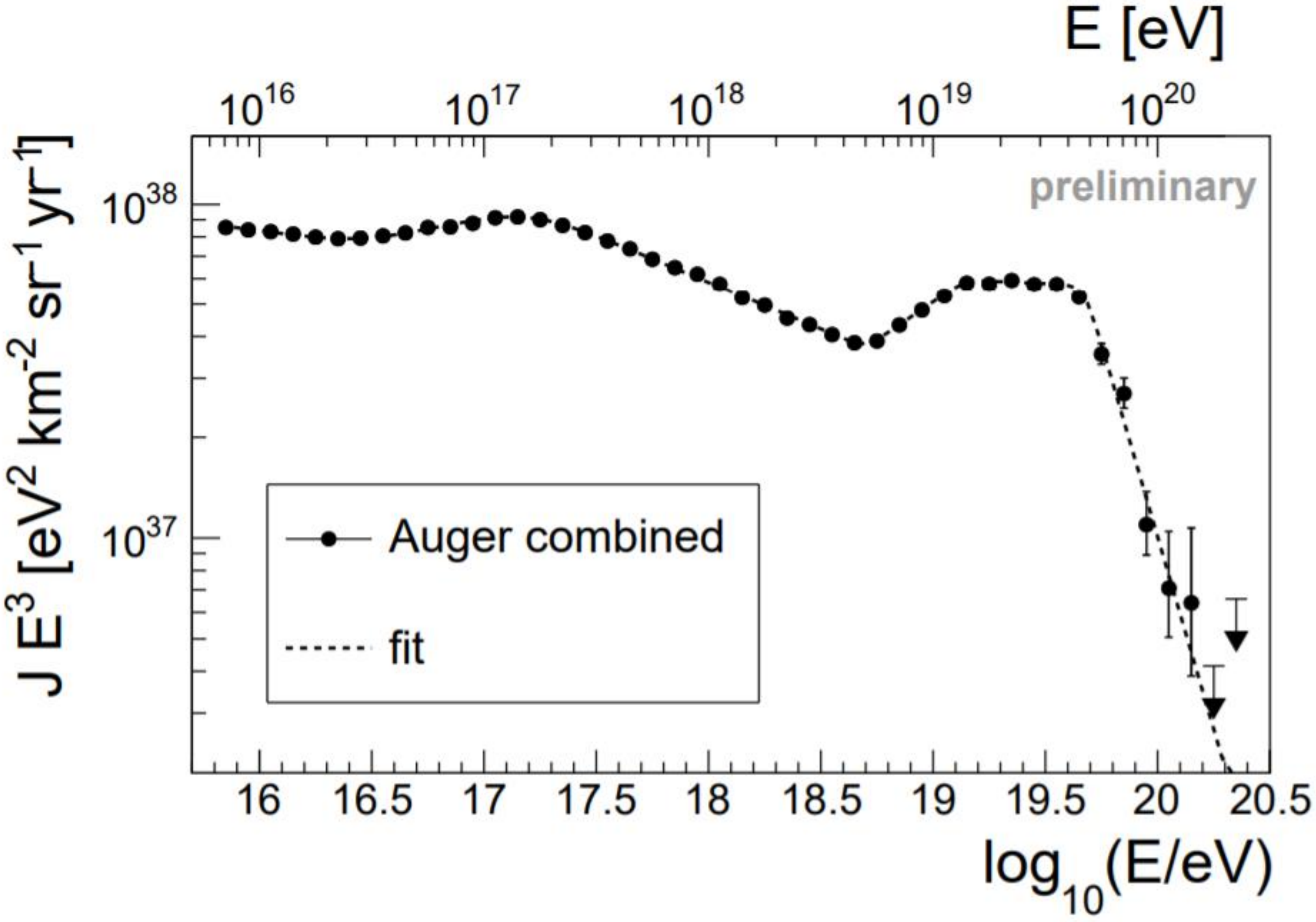

Accelerating cosmic rays

$$E_{max} = ZqBR_s$$

$$E_{max} = \varepsilon ZqBR_s$$
$$\varepsilon < 1$$

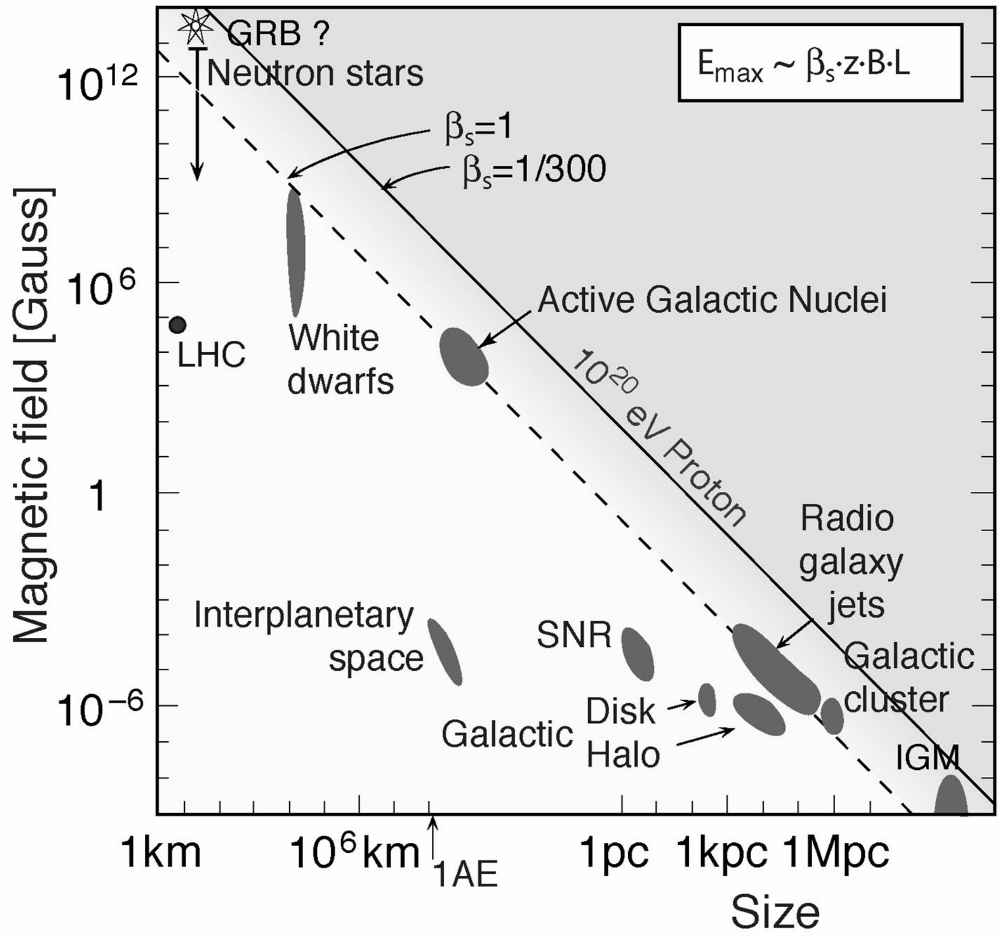

Dipole in lower energy bin 4-8 EeV

- Measured dipole in energy bin $(4-8)$ EeV is not significant $(< 3\sigma)$

  amplitude $2.5^{+1.0}_{-0.7}$ %

  direction $\alpha = (80 \pm 60)^{\circ}, \delta = (-24^{+12}_{-13})^{\circ}$

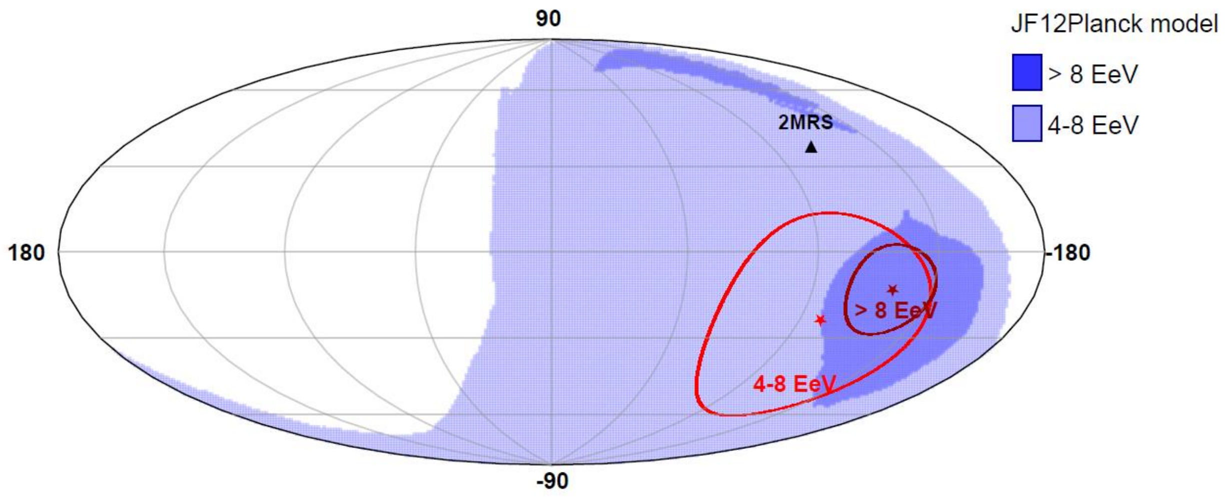

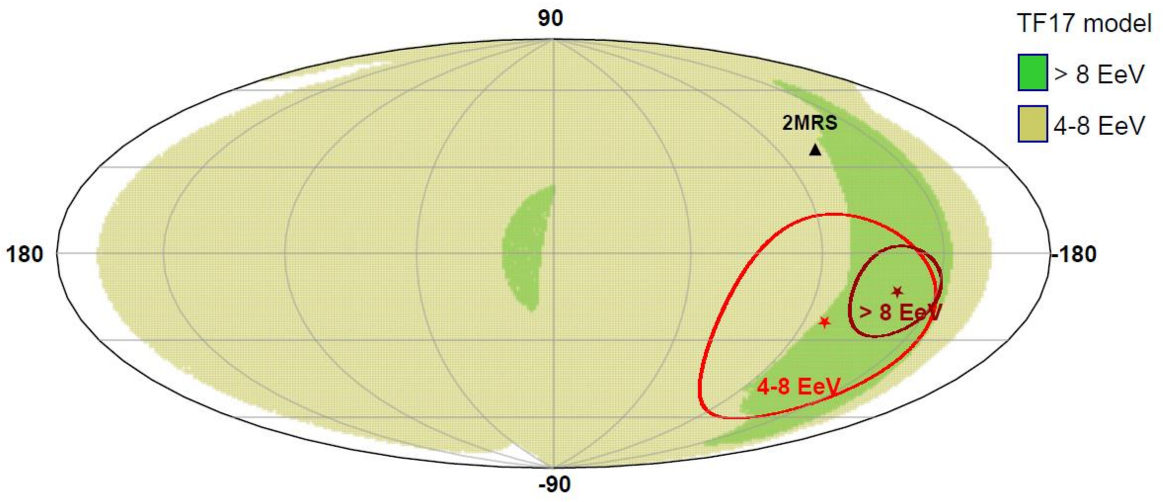

Spectral index

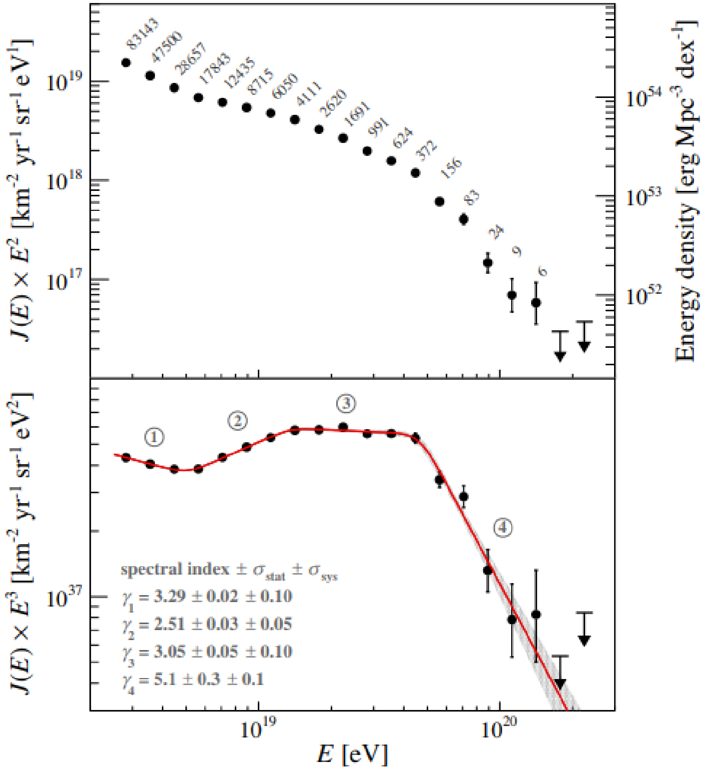

TABLE I. Spectral parameters in three different declination ranges. The energies E_{12}, E_{23}, and E_{34} are given in units of 10^{18} eV and the normalization parameter J_0 in units of 10^{18} km^{-2} sr^{-1} yr^{-1} eV^{-1}. Uncertainties are statistical.

	[−90.0°, −42.5°]	[−42.5°, −17.3°]	[−17.3°, +24.8°]
J_0	1.329 ± 0.007	1.306 ± 0.007	1.312 ± 0.006
γ_1	3.26 ± 0.03	3.31 ± 0.03	3.30 ± 0.03
γ_2	2.53 ± 0.04	2.54 ± 0.04	2.44 ± 0.05
γ_3	3.1 ± 0.1	3.0 ± 0.1	3.0 ± 0.1
γ_4	5.2 ± 0.4	4.4 ± 0.3	5.7 ± 0.6
E_{12}	5.1 ± 0.2	4.9 ± 0.2	5.2 ± 0.2
E_{23}	14 ± 2	14 ± 2	12 ± 1
E_{34}	47 ± 4	37 ± 4	51 ± 4

PHYSICAL REVIEW LETTERS **125,** 121106 (2020)

- All results obtained for spectral index -3 constant for the whole energy range – in reality the spectral index changes
- Results checked for spectral index -2.5 and -3.5 → small deviations of the resulting areas of allowed extragalactic directions of the dipole ~3°

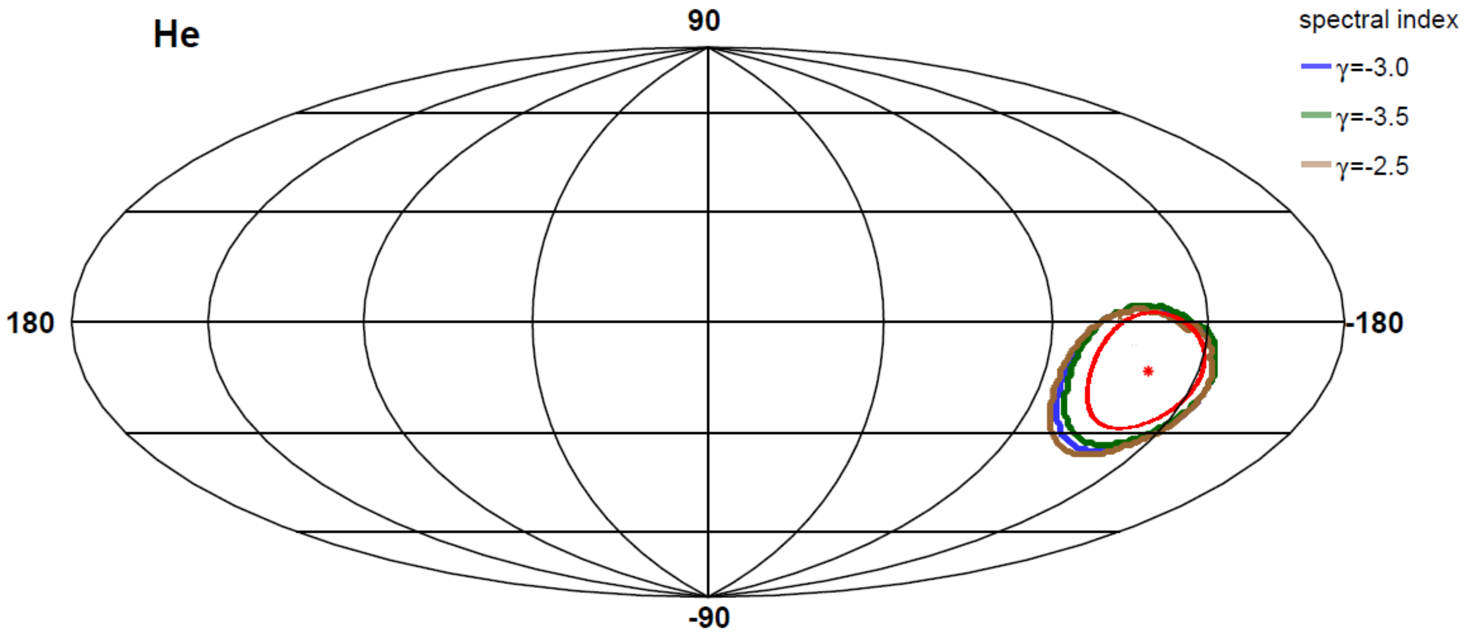

χ^2 checks in right ascension

- All solutions found for three dimensional dipole also checked in the distribution of arrival directions in the right ascension
- Fitted with dipole and dipole+quadrupole behavior
    - No significant quadrupole amplitudes

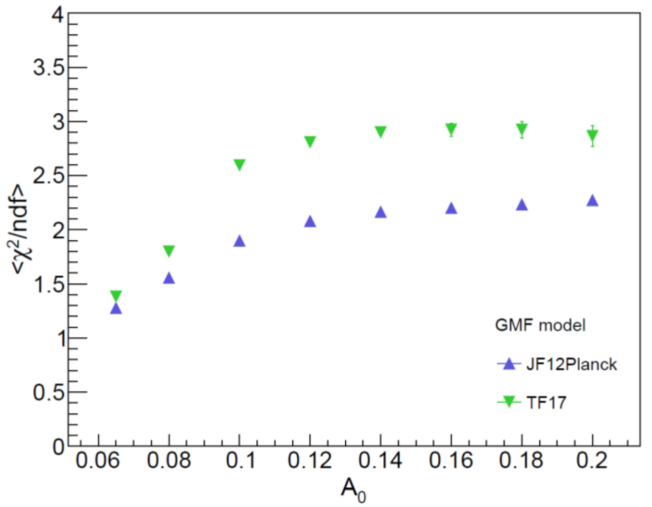

- Slight evolution of χ^2 with initial amplitude
- No significant evolutions of χ^2 with distance to measured dipole